Supporting Information

Synergistic W-Doping and Co_3S_4 Heterostructuring in NiFe LDH for Energy-Saving Hydrogen Production via Urea-Assisted Water Electrolysis

Zelin Yang [a], Peng Dai [a, *], Haoran Zhen [a], Tongtong Jiang [a, *], Kaiwen Wang [b], Mingzai Wu [a, *]

[a] School of Materials Science and Engineering, Anhui University, Hefei 230601, China.

[b] Stony Brook Institute at Anhui University, Anhui University, Hefei 230039, China.

[*] **Corresponding authors.**

E-mail addresses: daipeng@ahu.edu.cn (P. Dai), jtt@ahu.edu.cn (T. Jiang), wumz@ahu.edu.cn (M. Wu).

Experimental Section

1. Materials

Nickel nitrate ($Ni(NO_3)_2·6H_2O$ 99%), ferric nitrate ($Fe(NO_3)_3·9H_2O$ 98.5%), ammonium fluoride (NH_4F 99%), urea ($CO(NH_2)_2$ 99%), Potassium hydroxide (KOH 99%), phosphotungstic acid hydrate ($H_3O_{40}PW_{12}.xH_2O$，99%）Cobalt nitrate ($Co(NO_3)_2$ 99%) and Thiourea (CH_4N_2S 98%) were purchased from Aladdin Biochemical Technology Co., Ltd. 20 wt % Pt/C and Nafion (5%) were purchased from Shanghai Sigma-Aldrich Chemical Reagent Co., Ltd. Nickel foam (NF 99.8% 1.5 mm) was purchased from Tianjin Aiweixin Chemical Technology Co., Ltd. All materials were analytically pure and not further purified.

2. Experimental procedure

2.1 NF pretreatment

Nickel foam (NF, 3 × 4 cm) was ultrasonically cleaned with hydrochloric acid (3 M), ethanol and DI water for 15 minutes to remove surface oxides and impurities, dried in a vacuum drying oven at 60 °C for 6 hours.

2.2 Preparation of W-NiFe LDH/NF and NiFe LDH/NF

Firstly, 0.72 mmol of $Ni(NO_3)_2$, 0.36 mmol of $Fe(NO_3)_3$, 0.05 mmol $H_3O_{40}PW_{12}.xH_2O$, 2.5 mmol of NH_4F and 6 mmol of urea were dissolved in 60 mL of DI water and stirred for half-an-hour. Then, the solution and NF were placed into a 100 mL stainless steel high-pressure reactor and heated at 120 °C for 5 hours. The obtained W-NiFe LDH/NF was washed with DI water and ethanol to remove impurities and unstable nanosheets. NiFe LDH/NF can be obtained without adding $H_3O_{40}PW_{12}.xH_2O$ during the synthesis process.

2.3 Preparation of W-NiFe LDH@Co_3S_4/NF

First, dissolve 0.4 mmol of $Co(NO_3)_2·6H_2O$ and 0.2 mmol of CH_4N_2S in 60 mL of DI water. Subsequently, place the W-NiFe LDH/NF sample and the solution into a 100 mL high-pressure reactor, heating to 160°C and maintaining this temperature for 8 hours. The resulting sample was washed with DI water and ethanol, then dried in an oven to obtain W-NiFe LDH@Co_3S_4/NF.

Electrochemical measurements

All the electrochemical tests were carried out on a CHI-660E electrochemical workstation (Shanghai Chenhua Co. Ltd., China). A standard three-electrode system was used. An Ag/AgCl electrode and a graphite rod were used as the reference and counter electrodes, respectively. All samples were cut into 1 × 0.5 cm^2 and used as working electrodes. 1 M KOH solution was used as the electrolyte for HER tests. In the case of the UOR, the electrolyte was 1 M KOH + 0.33 M urea. A catalyst based on commercial Pt/C was used as the reference sample and the process is as follows: 10 mg of Pt/C was dispersed in 300 μl of isopropanol, 650 μl of DI water and 50 μl of Nafion solution by sonication for at least 30 min to form a homogeneous ink. 75 μl of catalyst ink was uniformly dripped onto the surface of 1 × 1.5 cm^2 NF and dried at room temperature and named Pt/C/NF. The measured potentials in this study were converted with respect to the reversible hydrogen electrode (RHE) according to the Nernst equation $E_{RHE} = E_{Ag/AgCl} + 0.197 + 0.059$ pH. Linear sweep voltammetry (LSV) was carried out at 10 mV s^{-1} for the polarization curves and Tafel slopes were calculated from the LSV curves. The electrochemical impedance spectra (EIS) were tested at a voltage amplitude of 5 mV over a frequency range of 10^5 Hz to 10^{-1} Hz at −1.3 V for the HER and 0.4 V for the UOR and OER.

Materials characterization

The image composition of the sample was determined by X-ray diffractometry and Cu Kα (λ = 0.15406 nm) radiation (XRD Bruker D8-ADVANCE). The surface morphology of the samples was observed using a scanning electron microscope (FE-SEM, Regulus 8230, Hitachi, Japan) and a transmission electron microscope (TEM, JEM-2100, JEOL, Japan). A scanning electron microscope equipped with an energy dispersive X-ray spectrometer (EDS) was used to estimate the fine structure. The chemical valence state of the sample was determined by X-ray photoelectron spectroscopy (XPS, ESCALAB 250Xi). All binding energies of elements were calibrated to a carbon binding energy of 284.8 eV. In-situ Raman spectra tests were collected using an in-situ Raman cell through a Raman microscope (iHR320

monochromator, HORIBA) with a S3 frequency-doubled Nd: YAG laser of 532 nm, and the spectra were collected using a grating of 1800 lines/ mm.

DFT Method

All the DFT calculations were conducted based on the Vienna Ab initio Simulation Package (VASP)[1-2]. The exchange-correlation potential was described by the Perdew−Burke−Ernzerhof (PBE) generalized gradient approach (GGA)[3]. The electron-ion interactions were accounted by the projector augmented wave (PAW)[4]. All DFT calculations were performed with a cut-off energy of 400 eV, and the 2×2×1 Monkhorst-Pack grid k-points were selected to sample the Brillouin zone integration. The energy and force convergence criteria of the self-consistent iteration were set to 10^{-5} eV and -0.05 eV $Å^{-1}$, respectively. DFT-D3 method was used to describe van der Waals (vdW) interactions [5].

The Gibbs free energy changes (ΔG) of the reaction are calculated using the following formula:

$$\Delta G = \Delta E + \Delta \mathrm{ZPE} - T\Delta S + \Delta G_{\mathrm{U}} + \Delta G_{\mathrm{pH}}$$

where ΔE is the electronic energy difference directly obtained from DFT calculations, ΔZPE is the zero-point energy difference, T is the room temperature (298.15 K) and ΔS is the entropy change. $\Delta G_{\mathrm{U}} = -eU$, where U is the applied electrode potential. $\Delta G_{\mathrm{pH}} = k_{\mathrm{B}}T \times \ln 10 \times \mathrm{pH}$, where k_{B} is the Boltzmann constant, and pH value is set to 0.

The adsorption energy (E_{ads}) is defined as:

$$E_{ads} = E_{complex} - E_{substrate} - E_{adsorbate}$$

where substrate and adsorbate refer to the substrate surface and adsorbate molecule, respectively. The smaller the adsorption energy, the more stable it is.

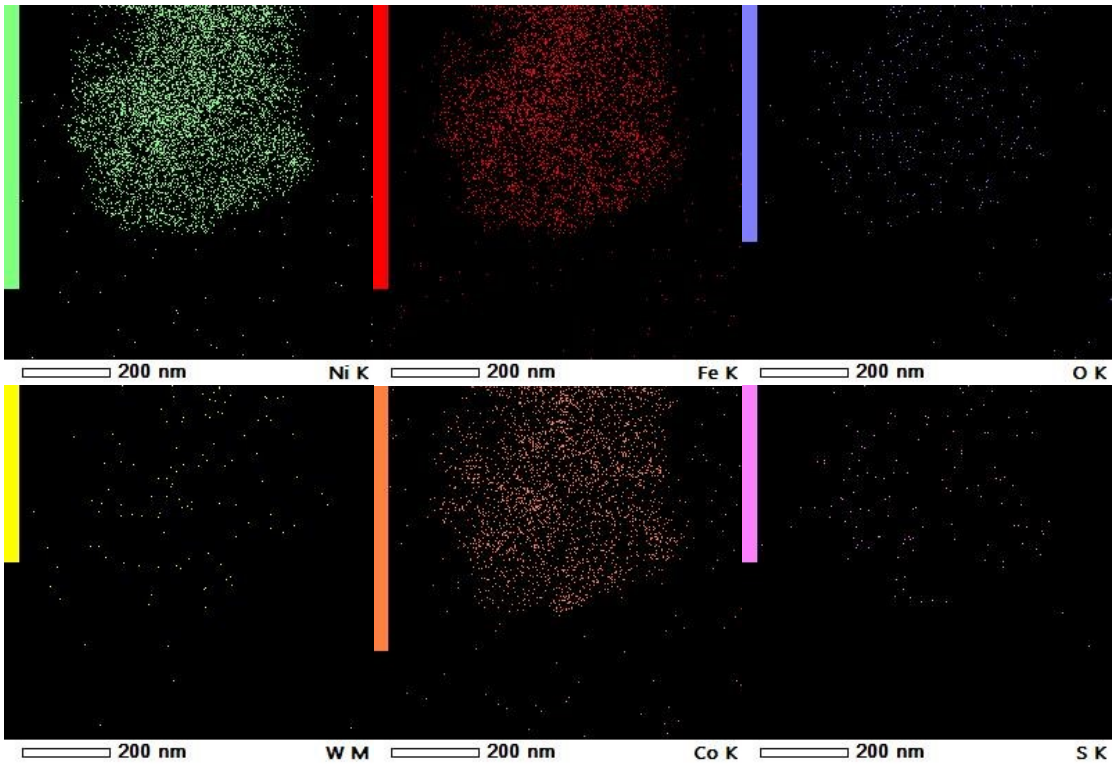

Fig.S1 EDS composition of each element of W-NiFe LDH@Co_3S_4/NF

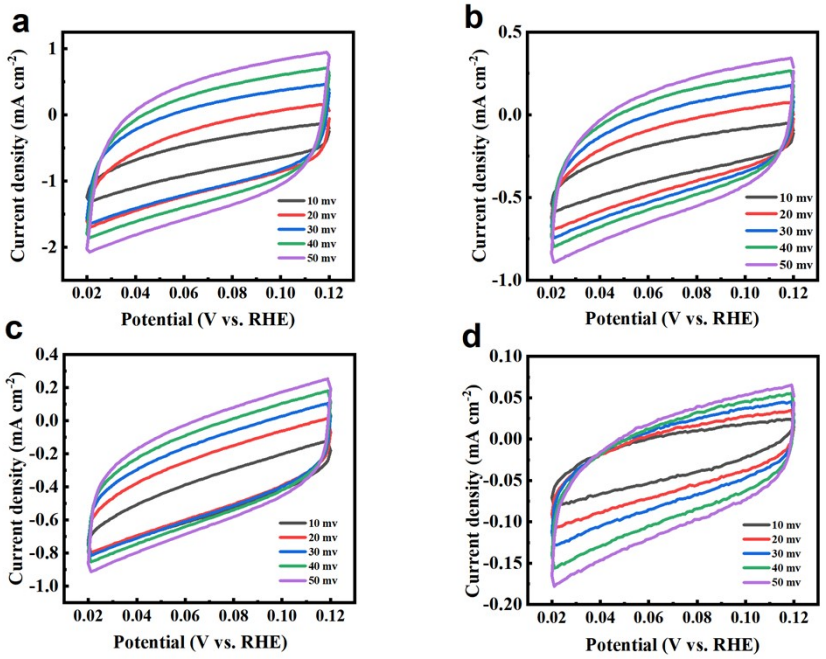

Fig. S2 CV curves of (a) W-NiFe LDH@Co_3S_4/NF, (b) NiFe LDH@Co_3S_4/NF, (c) W-NiFe LDH/NF and (d) NiFe LDH/NF in 1.0 M KOH + 0.33 M urea at scanning rates of 10, 20, 30, 40, and 50 mV s^{-1}.

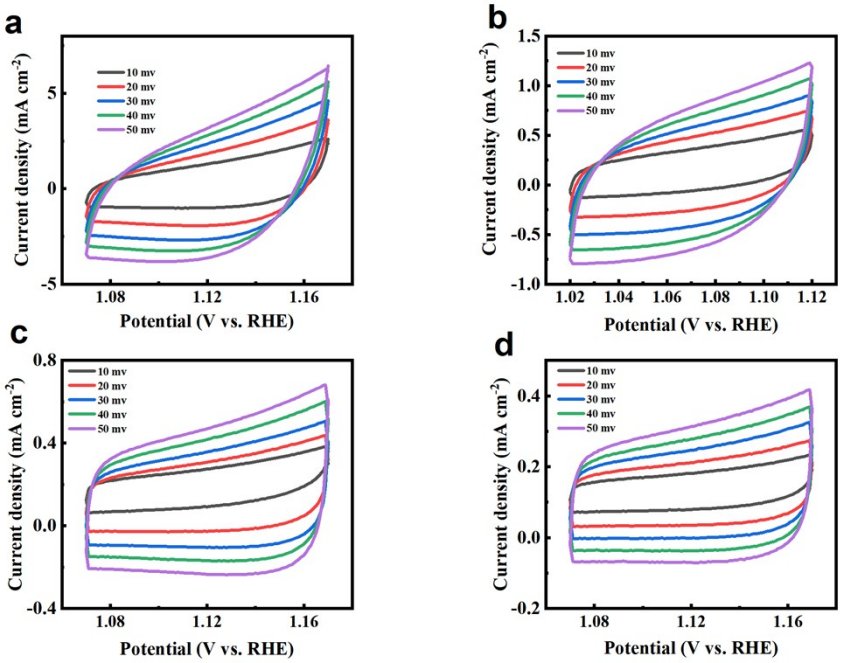

Fig. S3 CV curves of (a) W-NiFe LDH@Co_3S_4/NF, (b) NiFe LDH@Co_3S_4/NF, (c) W-NiFe LDH/NF and (d) NiFe LDH/NF in 1.0 M KOH at scanning rates of 10, 20, 30, 40, and 50 mV s^{-1}.

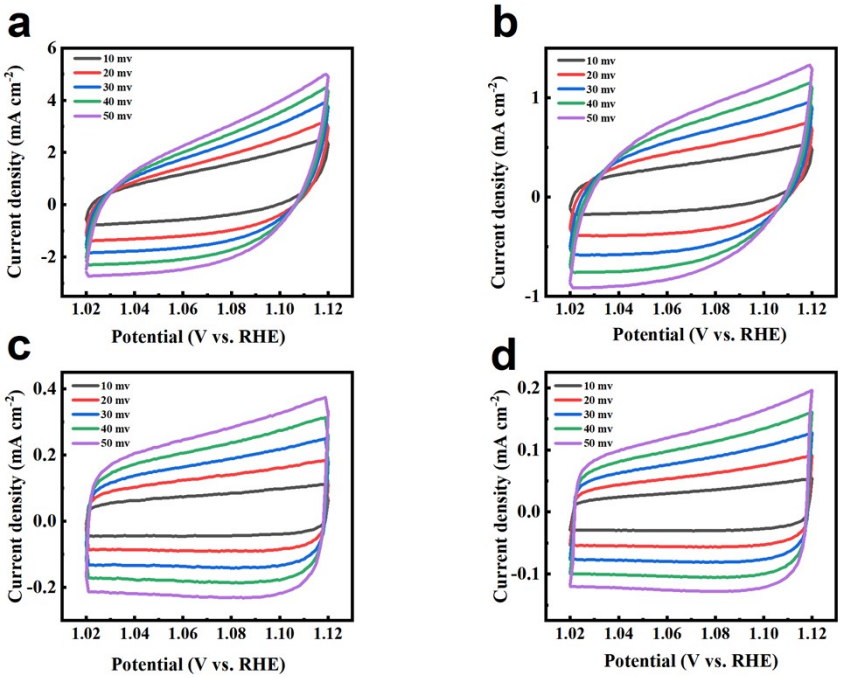

Fig.S4 CV curves of (a) W-NiFe LDH@Co_3S_4/NF, (b) NiFe LDH@Co_3S_4/NF, (c) W-NiFe LDH/NF and (d) NiFe LDH/NF in 1.0 M KOH + 0.33 M urea at scanning rates of 10, 20, 30, 40, and 50 mV s^{-1}.

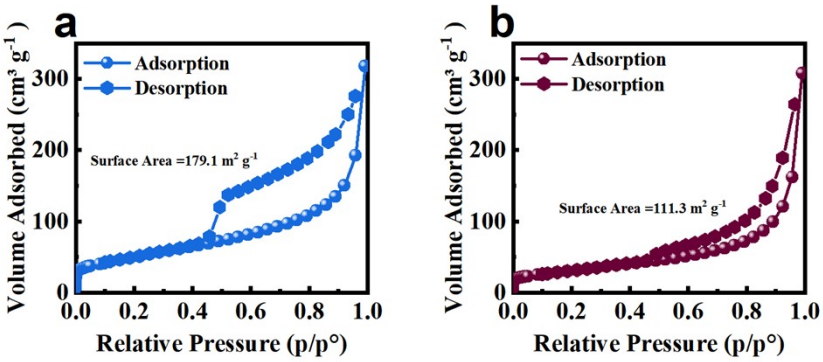

Fig.S5 N_2 adsorption-desorption isotherm of (a) W-NiFe LDH@Co_3S_4/NF and (b) W-NiFe LDH/NF.

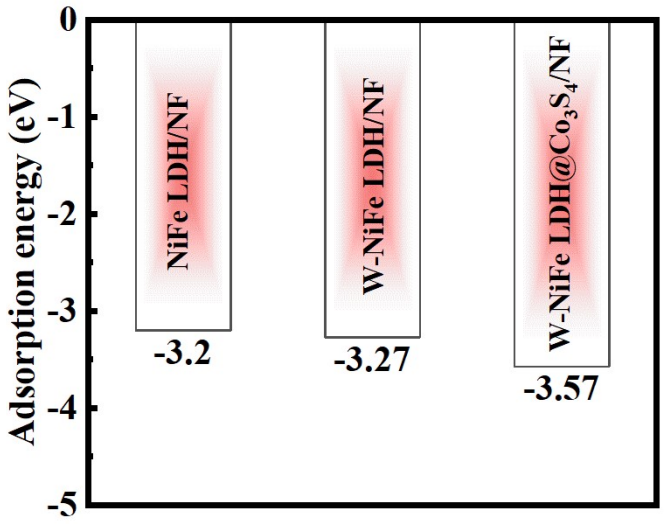

Fig.S6 H*Adsorption Energy for W-NiFe LDH@Co_3S_4/NF, W-NiFe LDH/NF and NiFe LDH/NF.

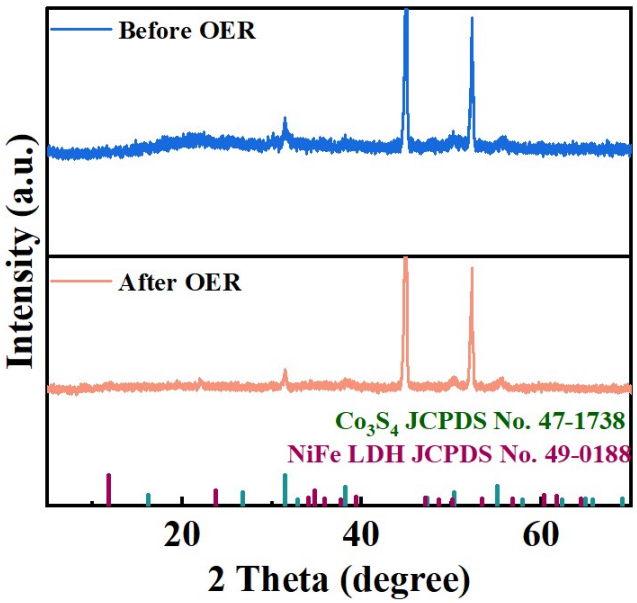

Fig.S7 The XRD of W-NiFe LDH@Co_3S_4/NF before and after OER CP testing.

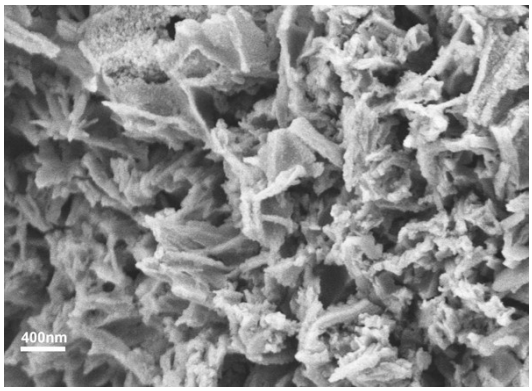

Fig.S8 The SEM of W-NiFe LDH@Co_3S_4/NF after OER CP testing.

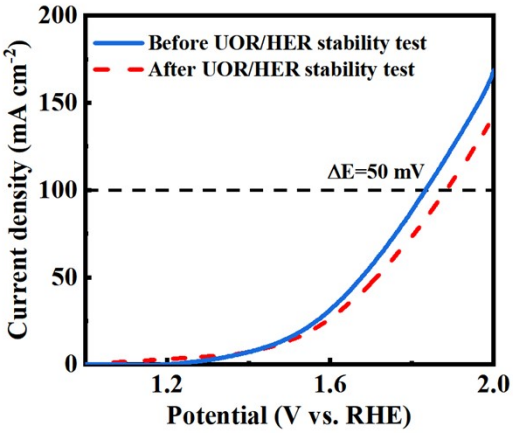

Fig.S9 The linear polarization curves of W-NiFe LDH@Co_3S_4/NF before and after UOR/HER stability test

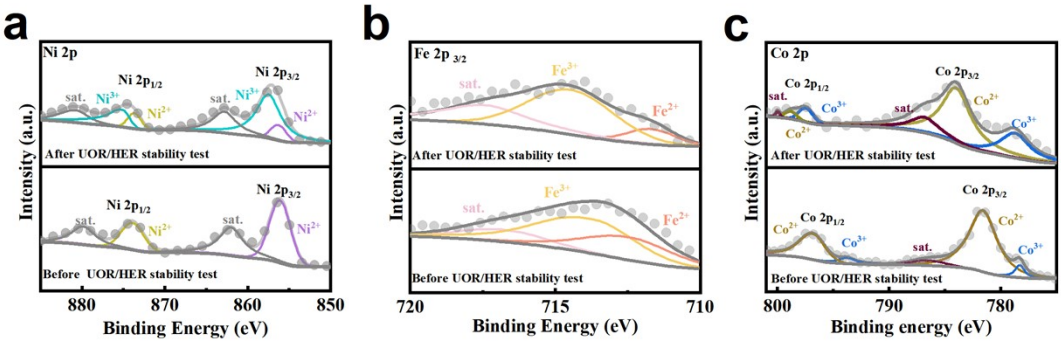

Fig.S10 (a) Ni, (b) Fe and (c) Co XPS for W-NiFe LDH@Co_3S_4/NF composite after UOR/HER stability test.

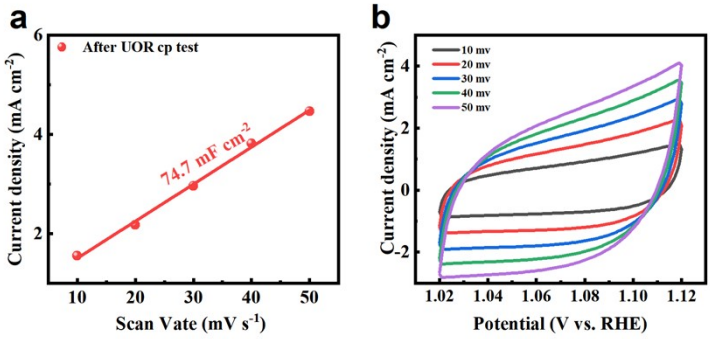

Fig. S11 (a) C_{dl} of W-NiFe LDH@Co_3S_4/NF and (b) CV curves at different scan rates in 1M KOH+0.33M Urea after UOR/HER CP testing.

Table S1 UOR performance comparison of reported catalysts in 1.0 M KOH+0.33 M urea

Sample	Potential @100 mA cm^{-2} (V vs. RHE)	Substrate	Refs.
W-NiFe LDH@Co_3S_4/NF	1.41	Ni foam	This work
NiFeRh-LDH	1.46	Ni foam	[6]
F-NiFe LDH	1.47	glassy carbon	[7]
NiMoV LDH	1.4	Ni foam	[8]
$NiWO_4$	1.42	Glassy carbon	[9]
La-Ni(OH)x	1.49	Ni foam	[10]
Ovac-V-$Ni(OH)_2$	1.47	Ni foam	[11]
$Ni(OH)_2$-$NiMoO_x$	1.43	Nickel foam	[12]
NiF_3/Ni_2P	1.57	Carbon cloth	[13]
W-Ni-$C_3S_3N_3$	1.43	Nickel foam	[14]

Table S2 Elemental content distribution of W-NiFe LDH@Co_3S_4/NF obtained based on XPS analysis.

Element	Ni	Fe	W	O	Co	S
Atomic (%)	26.89	0.81	0.05	62.47	4.02	5.76

Table S3 HER performance comparison of reported catalysts.

Sample	Overpotential @10 mA cm^{-2}	Substrate	Refs.
W-NiFe LDH@Co_3S_4/NF	**152**	Ni foam	This work
CoSe/NiFe LDH	260	Graphene foil	[15]
CoNi(OH)x	280	Cu foil	[16]
NiS-$Ni(OH)_2$ /MoSx /NF	226	Ni foam	[17]
$Ni(OH)_2$NSs	374	Glassy carbon	[18]
CoFe LDH	320	Ni foam	[19]
CoFe-LDH@g-C_3N_4	417	Glassy carbon	[20]
$Co_{0.4}Fe_{0.6}$ LDH/g-CNx	270	Glassy carbon	[21]
CoP@Co-Fe LDH	172	Carbon cloth	[22]

Table S4 OER performance comparison of reported catalysts in 1.0 M KOH.

Sample	Overpotential @100 mA cm^{-2}	Substrate	Refs.
W-NiFe LDH@Co_3S_4/NF	**299**	Ni foam	This work
Mo-doped CoFe LDH/NF	331	Ni foam	[23]
Ga−Ni_3S_2@ Ti_3C_2/NF	340	Ni foam	[24]
Co_9S_8-Ni_3S_2 NAs/NF	346	Ni foam	[25]
VO_x/Ni_3S_2@NF	358	Ni foam	[26]
NiCoS/NF	370	Ni foam	[27]
FeNi@FeNiB-700	399	Ni foam	[28]
CuCo-Ni_3S_2/NF-100	400	Ni foam	[29]
$NiCo_2O_4$−$NiCo(OH)_x$	484	Ni foam	[30]

Table S5 Comparison of recently reported urea electrolysis catalysts in alkaline media.

Sample	Electrolytes	Cell voltage (j=10 mA cm^{-2})	Refs.
W-NiFe LDH@Co_3S_4/NF	**1.0 M KOH + 0.33 M urea**	**1.44 V**	**This work**
CoMn/$CoMn_2O_4$	1.0 M KOH + 0.5 M urea	1.51 V	[31]
Ni-S-Se/NF	1.0 M KOH + 0.5 M urea	1.47 V	[32]
NiCoFe-LDH	1.0 M KOH + 0.33 M urea	1.49 V	[33]
Co-Ni_5P_4-NiCoOH	1.0 M KOH + 0.5 M urea	1.57 V	[34]
Fe-doped NiS–NiS_2	1.0 M KOH + 0.33 M urea	1.55 V	[35]
V-$Co_2P_4O_{12}$	1.0 M KOH + 0.5 M urea	1.42 V	[36]
$FeNi_2S_4$/CoFe	1.0 M KOH + 0.5 M urea	1.56 V	[37]
O-NiMoP/NF	1.0 M KOH + 0.5 M urea	1.55 V	[38]

References

1. G. Kresse and J. Hafner, Physical Review B, 1993, 47, 558-561.
2. G. Kresse and J. Hafner, Physical Review B, 1994, 49, 14251-14269.
3. K. B. John P. Perdew, Matthias Ernzerhof, Physical Review Letters, 1996.
4. G. K. D. Joubert, PHYSICAL REVIEW B, 1999, 1758-1775.
5. S. Grimme, J. Antony, S. Ehrlich, H.A. Krieg, J. Chem. Phys. 132 (2010), 154104.
6. H. Sun, W. Zhang, J.-G. Li, Z. Li, X. Ao, K.-H. Xue, K. K. Ostrikov, J. Tang and C. Wang, Applied Catalysis B: Environmental, 2021, 284.
7. K. Wang, M. Hou, W. Huang, Q. Cao, Y. Zhao, X. Sun, R. Ding, W. Lin, E. Liu and P. Gao, Journal of Colloid and Interface Science, 2022, 615, 309-317.
8. Z. Wang, W. Liu, J. Bao, Y. Song, X. She, Y. Hua, G. Lv, J. Yuan, H. Li and H. Xu, Chemical Engineering Journal, 2022, 430.
9. R. Lin, L. Kang, T. Zhao, J. Feng, V. Celorrio, G. Zhang, G. Cibin, A. Kucernak, D. J. L. Brett, F. Corà, I. P. Parkin and G. He, Energy & Environmental Science, 2022, 15, 2386-2396.
10. D. Li, X. Zhou, Q. Ruan, L. Liu, J. Liu, B. Wang, Y. Wang, X. Zhang, R. Chen, H. Ni, C. Huang, H. Wang and P. K. Chu, Advanced Functional Materials, 2023, 34.
11. H. Qin, Y. Ye, J. Li, W. Jia, S. Zheng, X. Cao, G. Lin and L. Jiao, Advanced Functional Materials, 2022, 33.
12. Z. Dong, F. Lin, Y. Yao and L. Jiao, Advanced Energy Materials, 2019, 9.
13. K. Wang, W. Huang, Q. Cao, Y. Zhao, X. Sun, R. Ding, W. Lin, E. Liu and P. Gao, Chemical Engineering Journal, 2022, 427.
14. M. Liu, W. Zou, S. Qiu, N. Su, J. Cong and L. Hou, Advanced Functional Materials, 2023, 34.
15. Y. Hou, M. R. Lohe, J. Zhang, S. Liu, X. Zhuang and X. Feng, Energy & Environmental Science, 2016, 9, 478-483.
16. X. Liu, S. Cui, Z. Sun, Y. Ren, X. Zhang and P. Du, The Journal of Physical Chemistry C, 2016, 120, 831-840.
17. T. Yoon and K. S. Kim, Advanced Functional Materials, 2016, 26, 7386-7393.

18. X. Sun, Q. Shao, Y. Pi, J. Guo and X. Huang, Journal of Materials Chemistry A, 2017, 5, 7769-7775.
19. R. Yang, Y. Zhou, Y. Xing, D. Li, D. Jiang, M. Chen, W. Shi and S. Yuan, Applied Catalysis B: Environmental, 2019, 253, 131-139.
20. M. Arif, G. Yasin, M. Shakeel, M. A. Mushtaq, W. Ye, X. Fang, S. Ji and D. Yan, Materials Chemistry Frontiers, 2019, 3, 520-531.
21. T. Bhowmik, M. K. Kundu and S. Barman, ACS Applied Energy Materials, 2018, 1, 1200-1209.
22. G. H. Choi, J. Moon, E. Song, S. Cho, K. W. Park and J. T. Park, International Journal of Energy Research, 2022, 46, 24633-24644.
23. G. Zhao, B. Wang, Q. Yan and X. Xia, Journal of Alloys and Compounds, 2022, 902, 163738.
24. R. Wang, Y. Yang, Z. Sun and X. Lu, International Journal of Hydrogen Energy, 2022, 47, 2958-2966.
25. Y. Zhou, S. Xi, X. Yang and H. Wu, Journal of Solid State Chemistry, 2019, 270, 398-406.
26. Y. Niu, W. Li, X. Wu, B. Feng, Y. Yu, W. Hu and C. M. Li, Journal of Materials Chemistry A, 2019, 7, 10534-10542.
27. K.-L. Yan, X. Shang, Z. Li, B. Dong, J.-Q. Chi, Y.-R. Liu, W.-K. Gao, Y.-M. Chai and C.-G. Liu, International Journal of Hydrogen Energy, 2017, 42, 17129-17135.
28. H. Yuan, S. Wang, X. Gu, B. Tang, J. Li and X. Wang, Journal of Materials Chemistry A, 2019, 7, 19554-19564.
29. J.-F. Qin, M. Yang, S. Hou, B. Dong, T.-S. Chen, X. Ma, J.-Y. Xie, Y.-N. Zhou, J. Nan and Y.-M. Chai, Applied Surface Science, 2020, 502, 144172.
30. G. Chen, D. Chen, J. Huang, C. Zhang, W. Chen, T. Li, B. Huang, T. Shao, J. Li and K. K. Ostrikov, ACS Applied Materials & Interfaces, 2021, 13, 45566-45577.

31. C. Wang, H. Lu, Z. Mao, C. Yan, G. Shen and X. Wang, Advanced Functional Materials, 2020, 30, 2000556.
32. N. Chen, Y.-X. Du, G. Zhang, W.-T. Lu and F.-F. Cao, Nano Energy, 2021, 81, 105605.
33. K. Patil, P. Babar, H. Bae, E. Jo, J. S. Jang, P. Bhoite, S. Kolekar and J. H. Kim, Sustainable Energy & Fuels, 2022, 6, 474-483.
34. Y. Wang, C. Zhang, X. Du and X. Zhang, Dalton Transactions, 2022, 51, 14937-14944.
35. S. Huang, Q. Zhang, P. Xin, J. Zhang, Q. Chen, J. Fu, Z. Jin, Q. Wang and Z. Hu, Small, 2022, 18, 2106841.
36. X.-W. Chang, S. Li, L. Wang, L. Dai, Y.-P. Wu, X.-Q. Wu, Y. Tian, S. Zhang and D.-S. Li, Advanced Functional Materials, 2024, 34, 2313974.
37. V. Maheskumar, K. Saravanakumar, Y. Yea, Y. Yoon and C. M. Park, International Journal of Hydrogen Energy, 2023, 48, 5080-5094.
38. H. Jiang, M. Sun, S. Wu, B. Huang, C.-S. Lee and W. Zhang, Advanced Functional Materials, 2021, 31, 2104951.